Available online at www.sciencedirect.com
SCIENCE DIRECT®
Biochimica et Biophysica Acta 1650 (2003) 10–21
BIOCHIMICA ET BIOPHYSICA ACTA
BBA
www.bba-direct.com

Kinetic and physical characterisation of recombinant wild-type and mutant human protoporphyrinogen oxidases

Mbulelo H. Maneli[a], Anne V. Corrigall[a], Horst H. Klump[b], Lester M. Davids[a], Ralph E. Kirsch[a], Peter N. Meissner[a,*]

[a] *Lennox Eales Porphyria Laboratories, MRC/UCT Liver Research Centre, Department of Medicine, University of Cape Town Medical School, K-floor, Old GSH Main Building, Observatory 7925, South Africa*
[b] *Molecular and Cell Biology, University of Cape Town, Rondebosch 7701, South Africa*

Received 27 February 2003; received in revised form 9 May 2003; accepted 13 May 2003

Abstract

The effects of various protoporphyrinogen oxidase (PPOX) mutations responsible for variegate porphyria (VP), the roles of the arginine-59 residue and the glycines in the conserved flavin binding site, in catalysis and/or cofactor binding, were examined. Wild-type recombinant human PPOX and a selection of mutants were generated, expressed, purified and partially characterised. All mutants had reduced PPOX activity to varying degrees. However, the activity data did not correlate with the ability/inability to bind flavin. The positive charge at arginine-59 appears to be directly involved in catalysis and not in flavin-cofactor binding alone. The $K_m s$ for the arginine-59 mutants suggested a substrate-binding problem. $T_{1/2}$ indicated that arginine-59 is required for the integrity of the active site. The dominant α-helical content was decreased in the mutants. The degree of α-helix did not correlate linearly with $T_{1/2}$ nor T_m values, supporting the suggestion that arginine-59 is important for catalysis at the active site. Examination of the conserved dinucleotide-binding sequence showed that substitution of glycine in codon 14 was less disruptive than substitutions in codons 9 and 11. Ultraviolet melting curves generally showed a two-state transition suggesting formation of a multi-domain structure. All mutants studied were more resistant to thermal denaturation compared to wild type, except for R168C.

Keywords: Variegate porphyria; Porphyria; Haem biosynthesis; R59W

1. Introduction

Protoporphyrinogen oxidase (PPOX) (EC 1.3.3.4), the penultimate enzyme in the haem biosynthetic pathway, catalyses the oxidation of protoporphyrinogen IX to protoporphyrin IX [1,2]. In eukaryotes, PPOX is an intrinsic protein of the inner mitochondrial membrane and requires molecular oxygen and a flavin cofactor (in most cases FAD), for this conversion. However, it is possible that diverse catalytic mechanisms may exist, especially in prokaryotes that can survive under both aerobic and anaerobic conditions [3,4]. Three molecules of oxygen, whose ultimate fate is hydrogen peroxide rather than water, serves as the final electron acceptor in the aerobic reaction in both eukaryotic and prokaryotic PPOXs [5,6]. The reaction proceeds via three, two-electron oxidations rather than a single, six-electron oxidation (Dailey, H.A., personal communication). A mechanism for the removal of the four hydrogens in the *meso* positions of the porphyrin ring has been suggested in which three desaturation steps occur, with the involvement of one particular face of the porphyrin ring, and one prototropic-rearrangement step using the other face of the ring [7,8].

Sequence analysis of protein databases suggested that PPOXs are members of a protein superfamily that includes plant and animal phytoene desaturases and animal monamine oxidases [9]. These proteins all share significant sequence homology at the N terminus in a 60-amino-acid residue stretch that includes the dinucleotide cofactor binding motif.

PPOX has been purified from the mitochondria of mouse liver [10,11], yeast [3], ox [12], barley [13], maize [14] and spinach chloroplasts [15]. In addition to purification from

* Corresponding author. Tel.: +27-21-406-6206; fax: +27-21-448-6815.
E-mail address: PETE@LIVER.UCT.AC.ZA (P.N. Meissner).

1570-9639/03/$ - see front matter © 2003 Elsevier B.V. All rights reserved.
doi:10.1016/S1570-9639(03)00186-9

these sources, human PPOX has been cloned, expressed and purified [16,17]. The human enzyme is a homodimer and contains one noncovalently bound FAD per dimer [16]. Yeast PPOX also contains FAD and, furthermore, it has been suggested that there are essentially two domains in the protein structure defined by a single protease digestion site, the N-terminal domain containing the FAD binding fold and the C-terminal domain containing the active site at the interface between it and the N-terminal domain [18].

A group of herbicides, the diphenylethers (DPEs), are good inhibitors of PPOX and provide a useful tool to investigate the substrate binding site/catalysis of the enzyme. They are competitive inhibitors (with respect to the tetrapyrrole substrate protoporphyrinogen IX) of plant, mouse and human PPOX [19,20]. However, this inhibition by DPEs is not seen in all PPOXs, e.g., *B. subtilis*, *E. coli* and *B. japonicum* PPOXs [21–23] are not inhibited by these herbicides. In plants, this inhibition induces light-dependent phytotoxic damage through induction and accumulation of protoporphyrin IX in the exposed plant, and engineered overproduction of PPOX in plants may confer resistance towards these herbicides [24,25]. An important feature of these inhibitors is that their structure mimics half of that of protoporphyrinogen IX. It could also be expected that certain other tetrapyrrolic compounds may also inhibit PPOX. Indeed, haem and its metabolic products bilirubin IX and biliverdin IX are also effective inhibitors of PPOX [1,23,26].

In humans, a defect in PPOX, resulting in approximately 50% decreased activity, is responsible for the dominantly inherited disorder; variegate porphyria (VP) [27–29]. The disease is characterised by an abnormal pattern of porphyrin excretion, and clinical manifestations include photosensitive skin lesions and/or a propensity to develop acute neurovisceral crises [28,30]. South Africa has the highest incidence of VP in the world, attributed to a founder effect, resulting from a mutation, R59W, in exon 3 of the PPOX gene [31,32]. Nine other mutations have also been reported in South Africa to date (R168C, H20P, 537delAT, Y348C, R138P, 769delG; 770T>A, L15F, G375X and V290M) in addition to the common R59W mutation [31–35]. Furthermore, heterogeneity of PPOX variants has been demonstrated worldwide with over 100 mutations identified [36–40]. The human *PPOX* gene contains 13 exons and is located on chromosome 1q22–23 [41–43].

To date, the direct effect of a number of mutations on PPOX activity in VP has been investigated. In some of these studies, activity of expressed mutant PPOX has been determined by direct fluorescence assay [31,44]. In others, PPOX activity was also screened for by complementation of the *E. coli* strain SAS38X, which lacks PPOX activity [45,46].

Missense mutations may directly affect substrate specificity, binding, stability or electronic catalysis, the ability to bind and utilise the FAD cofactor, or the ability to translocate to the mitochondria or the correct compartment within. As outlined above, exogenous compounds may also act as potent inhibitors of PPOX. Because all these factors may ultimately impair normal porphyrin and haem biosynthesis, their study may yield important insights into VP. Here, we compare some kinetic and physical characteristics of expressed wild-type and mutant PPOXs. A pTrcHis plasmid containing wild-type PPOX was expressed and purified. A selection of both naturally occurring mutants relevant to South Africa (H20P, R59W, R168C and Y348C) and certain self-designed mutants were constructed. We examined the relevance of the positively charged R59 residue and the role of glycine residues in the highly conserved "GXGXXG" FAD binding motif [16,17,47] in these mutants.

2. Materials and methods

2.1. Materials

The recombinant plasmid (pHPPO-X) was a gift from H.A. Dailey, University of Georgia, Athens, GA, USA. The GeneEditor kit was obtained from Promega, Madison, WI, USA and the oligonucleotides used to construct the mutants from Integrated DNA Technologies Inc., Coralville, IA, USA. Automated direct sequencing was performed on an ADI 3100 Automated Genetic Analyser using a Big Dye Version 3 kit (Applied Biosystems, Brachburg, NJ, USA). The sonicator utilised (Model XL2020) was obtained from Heat Systems, Framington, NY, USA. TALON resin was purchased from Clontech, Palo Alto, CA, USA. Acifluorfen (AF) and methyl acifluorfen (MeAF) were obtained from Chem Services, West Chester, PA, USA, and biliverdin IX hydrochloride (BV) and bilirubin IX (BR) from Porphyrin Products, Logan, USA. The Hybaid Omnigene thermal cycler was from Teddington, UK. Spectrophotometric measurements were performed on a Hitachi spectrophotometer and all fluorimetric measurements on a Hitachi 650-10S fluorescence spectrophotometer, Koki Co. Ltd., Japan. CD spectra were measured on a Jasco J-810 spectropolarimeter, Jasco Corporation 2967-5, Ishikawa-Cho, Hachioji-Shi, Tokyo 192, Japan. All thermal denaturation experiments were performed on a Pye-Unicam SP 1800 spectrophotometer with a custom-made heating block interfaced to an IBM-PC through an Oasis digital convertor.

2.2. Methods

2.2.1. Site-directed mutagenesis

The mutants were engineered from the recombinant plasmid (pHPPO-X) by site-directed mutagenesis using the GeneEditor kit according to manufacturer's instructions. Where possible, colonies were screened by restriction analysis (Table 1). Mutations were confirmed by automated direct sequencing and the entire *PPOX* cDNA was sequenced to ensure the absence of any erroneous mutations.

Table 1
Oligonucleotides used in site-directed mutagenesis

PPOX	Mutation oligonucleotides (5'→3')	Direction of oligonucleotides	Restriction enzymes
	S Y H L S R		
Wild type	CG GCT CAG GTG GTA ACT GGC		
	S Y **P** L S R		
H20P	5' Phos-CG GCT CAG GGG GTA ACT GGC	Reverse	None
	I V Y D S		
Wild type	GA ATC GTG TAT GAC TCA G		
	I V **C** D S		
Y348C	5' Phos-GA ATC GTG TGT GAC TCA G	Forward	MaeIII
	E L G P R G I R P		
Wild type	T GAG CTT GGA CCT CGG GGA ATT AGG CCA G		
	L G P **W** G I		
R59W	5' Phos-CTT GGA CCT TGG GGA ATT AG	Forward	AvaI
	E L G P **K** G I R P		
R59K	5' Phos-T GAG CTT GGA CCT AAG GGA ATT AGG CCA G	Forward	AvaI
	E L G P **S** G I R P		
R59S	5' Phos-T GAG CTT GGA CCT AGT GGA ATT AGG CCA G	Forward	AvaI
	E L G P **I** G I R P		
R59I	5' Phos-T GAG CTT GGA CCT ATT GGA ATT AGG CCA G	Forward	AvaI
	V V L G_9 G G_{11} I S G_{14} L A A		
Wild type	GTC GTG CTG GGC GGA GGC ATC AGC GGC TTG GCC GCC AG		
	V V L **A** G G I		
G9A	5' Phos-GTC GTG CTG GCC GGA GGC ATC	Forward	Eae1
	G G **A** I S		
G11A	5' Phos-TG GGC GGA GCC ATC AGC GG	Forward	Xcm I
	G I S **A** L A A		
G14A	5' Phos-GA GGC ATC AGC GCC TTG GCC GCC AG	Forward	MspA1 I

In each case the mutated DNA bp are underlined. The amino acids encoded by the sequences are shown above and the altered amino acids shown in bold. All oligonucleotides were 5′ phosphorylated. Restriction enzymes utilised for screening are shown on the right.

2.2.2. Expression and purification of human wild-type and mutant PPOX

pHPPO-X was initially transfected into and maintained in JM109 *E. coli* cells [16], as were the various mutants. JM109 cells (0.5 ml of a 30% glycerol stock) containing wild-type or mutant recombinants were inoculated into 1-l Luria broth containing 100 μg/ml ampicillin and incubated for 18 h at 30 °C on a rotary shaker (225 rpm). Cells were harvested by centrifugation (3000 × *g*) for 30 min at 4 °C and the entire purification performed at 4 °C. The pellet was resuspended in 30-ml sonication buffer (0.02 M Tris/HCl, 0.3 M NaCl, 0.01 M Imidazole, 1% (w/v) *n*-octyl-β-D-glucopyranoside, pH 8.0). The cells were sonicated at 3 × 30 s with intermittent cooling in ice water. The lysate was then centrifuged at 105 000 × *g* for 30 min at 4 °C and the supernatant retained. The supernatant was loaded onto 1 ml of TALON resin, pre-equilibrated in 10-ml sonication buffer, at 0.25 ml/min (or 0.4 ml/min in the case of R168C and Y348C). The column was washed with 10-ml 0.02 M Tris/HCl, 0.3 M NaCl, 0.02 M imidazole, 0.2% (w/v) *n*-octyl-β-D-glucopyranoside, pH 8.0 at 0.5 ml/min, prior to elution in elution buffer (0.02 M Tris/HCl, 0.3 M NaCl, 0.2 M imidazole, 0.2% (w/v) *n*-octyl-β-D-glucopyranoside, pH 8.0). PMSF was added to all buffers to a final concentration of 1 μg/ml throughout the purification procedure. Enzyme purity was confirmed on SDS-PAGE [48]. Protein concentration was determined by the Bio-Rad Protein assay [49] with BSA as protein standard.

2.2.3. PPOX assay

PPOX activity was measured by fluorescence as described previously [29]. The assay was performed at pH 8.2 except for Y348C, which had a pH optimum of 7.8.

2.2.4. Inhibitor studies and determination of kinetic data

Inhibition studies were performed as described previously [20] using AF, MeAF, BV and BR. IC_{50} was determined by measuring PPOX activity over a range of inhibitor concentrations at a single substrate concentration of 15 μM.

2.2.5. Determination of kinetic constants

The kinetic constants K_m and k_{cat} were determined from substrate-velocity plots, and the constants K_i and α and model discriminations from secondary replots of K_m/V_{max} vs. [AF] and $1/V_{max}$ vs. [AF], where K_m and V_{max} are the values determined in the presence of inhibitor (AF). Calculated K_i*s* were obtained by applying the relationship below, which exists for competitive inhibition between K_i, K_m and IC_{50} at any saturating substrate concentration, *S*:

$$K_i = \frac{IC_{50}}{(S/K_m) + 1} \quad (1)$$

2.2.6. FAD binding studies

To analyse the potential effects of the mutations on FAD binding to the protein, PPOX UV/VIS spectra were recorded from 250 to 550 nm for both wild type and mutants under identical conditions, in elution buffer, at room temperature. The FAD content was then obtained by measuring absorption at the maximum wavelength (450 nm) and expressed as absorption/mg protein/ml.

2.2.7. Effect of temperature on PPOX activity

Homogeneous wild-type and mutant PPOXs were divided into aliquots and each aliquot denatured in a thermal cycler at a specific temperature for 3 min and kept on ice. The temperatures ranged from 30 to 65 °C in 5 °C steps. One aliquot was not heat-denatured and was used as a reference. PPOX activity was assayed and the temperature that reduces enzyme activity to half its maximal velocity ($T_{1/2}$) determined from the plot of residual activity vs. temperature.

2.2.8. Thermal induced denaturation

Thermal denaturation experiments were performed in 0.01 M Tris–acetate, 0.2% (w/v) *n*-octyl-β-D-glucopyranoside, pH 7.2 at a PPOX concentration of 0.15 mg/ml on a spectrophotometer with a heating block. Temperature was increased from 15 to 75 °C at a rate of 1 °C/min. To investigate the effects of either AF or FAD on T_m, melting curves were generated at an enzyme/AF or FAD molar ratio of 1:1, 1:5, 1:10 and 1:20.

To assess the reversibility of folding, PPOX was heated at 75 °C (past the unfolding temperature) and cooled to an initial temperature of 15 °C before reheating back to 75 °C.

To determine the stability of folding domains, PPOX was heated to a temperature just below the T_m value and cooled to 15 °C, before reheating back to 75 °C.

Melting curves were analysed as described previously [50] and the temperature at which 50% of the protein is denatured (T_m) determined.

2.2.9. Circular dichroism

CD spectra of wild-type and mutants (0.15 mg/ml, in 0.01 M Tris–acetate, 0.2% (w/v) *n*-octyl-β-D-glucopyranoside, pH 7.2) were measured on a spectropolarimeter using a 0.1-cm path length quartz cuvette. All spectra were analysed by a 10-spectrum accumulation at room temperature. The secondary structure was estimated using computer software [51].

3. Results and discussion

3.1. Expression and purification of human wild-type and mutant PPOX

Talon metal affinity chromatography of the supernatant from 30-ml sonicate of expressed wild-type or mutant PPOX yielded pure enzyme, M_r 51 000, as judged by SDS-PAGE (data not shown), in all cases. No IPTG induction scheme was followed, as it was found that growth into stationary phase was sufficient for good production of wild-type PPOX without IPTG, and IPTG did not improve expression of the mutant PPOXs. Maximum expression was obtained with incubation at 30 °C for 18 h (data not shown). Using these conditions, the formation of recombinant protein inclusion bodies, which can result from overexpression [52], was not apparent. All purifications were performed at 4 °C, as attempted purification of mutant PPOX at room temperature was problematic. The yields varied considerably and were lower than wild type in all mutants except for R59S where the yields were similar (Table 2). This variation may be explained by observed differences in binding affinities for the resin and/or the fact that mutant proteins frequently are more poorly expressed and unstable and undergo proteolytic cleavage in the cell [53]. In most cases the yield of purified PPOX was sufficient to assay and determine kinetic parameters. However, in the case of H20P, G9A and G11A, only specific activity could be measured due to a combination of low yield and activity.

3.2. PPOX activity

Table 2 lists both the specific activity (nmol/mg protein/min) for wild-type and mutant PPOXs. Y348C and R168C showed some residual activity, 8% and 17% of wild-type PPOX activity, respectively, whereas for R59W and the H20P the activity was negligible.

Interestingly, both the Y348C and R168C mutations were originally identified in compound heterozygote individuals, i.e., they have one of these mutations in addition to the common South African R59W mutation. Although these patients are clinically severely affected, the fact that they survive suggests that at least this level of residual PPOX activity, together with the negligible R59W activity, is compatible with life, as has been suggested previously [31,34,45].

In spite of what could be predicted as a relatively severe replacement (the additional cysteine residues may cross-react to form disulfide linkages) and that R168 lies within the putative membrane-anchoring domain [54], our activity

Table 2
Purification yield and activity of wild-type and mutant PPOXs

PPOX	Yield of PPOX from 1 l of culture (mg)	Specific activity (nmol/mg/min)	Percentage of wild-type activity
Wild type	2.00	7150.00 ± 192	100.00
Y348C	0.60	617.00 ± 8.97	8.63
R168C	0.40	1257.00 ± 41.4	17.50
H20P	0.03	11.32 ± 0.75	0.16
R59W	0.78	19.75 ± 1.05	0.28
R59K	1.51	2690.00 ± 66.7	37.60
R59S	2.21	183.10 ± 11.0	2.60
R59I	1.65	106.00 ± 7.27	1.50
G9A	0.12	36.85 ± 2.90	0.52
G11A	0.03	1.57 ± 0.14	0.02
G14A	0.69	3044.00 ± 67.2	42.60

results demonstrate that both R168C and Y348C have catalytic activity an order of magnitude greater than that of R59W. On the other hand, a recent report [46], demonstrated that R168H had negligible activity in spite of a relatively conservative replacement. This underlines the necessity to exercise caution in predicting the effects of specific mutations in PPOX.

The loss of activity with the H20P mutant suggests that PPOX is sensitive to structural change. The activity is severely affected, probably because it involves substitution of a positively charged amino acid, histidine, by a hydrophobic amino acid, proline. Proline residues have the propensity to form reverse turn structures in which its ring structure fits well and decreases protein flexibility by disruption of α-helices [55]. In addition, the H20P falls in the putative dinucleotide binding site and occurs immediately adjacent to a conserved lysine (K21).

The common South African founder mutation, R59W [31,32], falls within the 60-bp flanking region of the putative FAD dinucleotide binding motif of PPOX [9]. This makes it attractive to speculate that this may account for the severe loss of enzyme activity of the R59W. The UV/VIS spectra of the FAD bound to R59W PPOX demonstrate binding to be dissimilar to that of the wild type. It would appear that the mutant R59W may bind some FAD, but its interaction with the protein is compromised (Fig. 1). However, the possibility that the positive charge is required for oxidoreducto catalysis and/or substrate binding rather than, or in addition to, FAD binding, must be considered.

In order to study the relevance of the R59, we introduced both a conservative and two nonconservative replacements: R59K (positive to positive replacement), R59S (polar replacement) and R59I (aliphatic, neutral replacement). R59K resulted in considerably less disruption (37% of wild type activity) than when the charge was removed (< 3% of wild-type activity, for R59S and R59I) (Table 2). The observation that these nonconservative substitutions resulted in almost complete loss of PPOX activity underlines the requirement of a positive charge in codon 59. Both conservative and nonconservative replacements in this position appeared to bind FAD although in R59W, binding was reduced (Fig. 1). This suggests that R59 is required for catalytic activity (either directly or via impaired substrate binding) and the fact that FAD binding is reduced in the R59W mutant is due to the bulky nature of the aromatic tryptophan rather than the loss of the positive charge. Hydrophobicity at this position would appear to be unimportant for FAD binding as both R59I and R59W are hydrophobic replacements, yet differed in their ability to bind FAD.

PPOX exhibits a highly conserved GXGXXG motif (where X denotes any residue) at the N terminus, which is recognised as a signature sequence in a large number of dinucleotide-containing proteins. Crystallographic studies performed on other flavoproteins confirm the involvement of these residues in FAD binding and show the GXGXXG motif to be structurally enclosed in an ADP type-binding βαβ-fold [56–58]. In order to study the role of these glycine residues, we replaced the glycine residues at positions 9, 11 and 14 by alanine to produce the G9A, G11A and G14A mutations, respectively. Our results showed that substitution of glycine by alanine in codon position 14 resulted in less disruption (G14A activity, 43% of wild-type activity) than in codons 9 and 11 (G9A and G11A activity, < 1%). Other workers have investigated the importance of the glycine in the 1st, 3rd and 6th positions of the GXGXXG motif. Our results are in agreement with those of Nishiya and Iminaka [59] who mutated these glycines in *Athrobacter* sarcosine oxidase to alanine. They showed that substitution at positions 1 and 3 of the motif sequence was highly significant, and at the 6th position less so. Clearly these glycines are critical for structural maintenance of the dinucleotide binding site and consequent activity of the protein.

The "X" residues are much less important. Nishiya and Iminaka [59] examined the frequencies of amino acids appearing in the GXGXXG motif. Apart from the three highly conserved glycines, only the first X showed any clear tendency, in that glycine and alanine appeared in approximately 42% of the 133 sequences of the FAD or NAD-dependent proteins studied. It was noted that overall, large amino acids were infrequent and the frequencies of basic, acidic and aromatic amino acids were especially low.

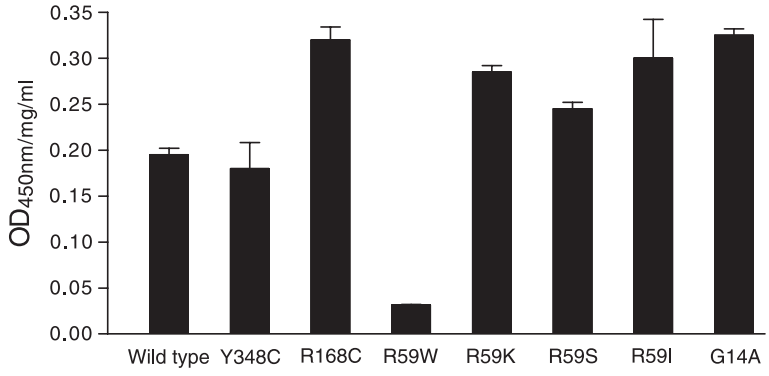

Fig. 1. FAD absorption at 450 nm for wild-type and mutant PPOXs.

Table 3
Substrate binding affinity and catalytic efficiency of wild-type and mutant PPOXs

PPOX	K_m (μM)	k_{cat} (s^{-1})	k_{cat}/K_m (s^{-1} μM^{-1})
Wild type	0.85 ± 0.09	5.95 ± 0.44	7.00
Y348C	1.07 ± 0.09	0.53 ± 0.07	0.50
R168C	1.00 ± 0.06	1.02 ± 0.03	1.02
H20P	ND	ND	ND
R59W	1.26 ± 0.10	0.04 ± 0.01	0.03
R59K	0.83 ± 0.09	2.57 ± 0.12	3.10
R59S	1.70 ± 0.24	0.17 ± 0.01	0.10
R59I	2.09 ± 0.06	0.15 ± 0.01	0.07
G9A	ND	ND	ND
G11A	ND	ND	ND
G14A	0.85 ± 0.03	3.90 ± 0.15	4.59

ND = not determined.

3.3. Kinetics of wild-type and mutant PPOXs

For human PPOX the oxidation of protoporphyrinogen IX to protoporphyrin IX obeyed Michaelis–Menten kinetics (data not shown). This is in keeping with all other kinetic profiles reported for other PPOX species [3,20,23]. Differences in the reported kinetic constants between the different species of PPOX presumably reflect differences in their substrate (and/or inhibitor) binding abilities, which have arisen over time in response to evolutionary factors. A complete set of kinetic data could not be determined for mutants H20P, G9A and G11A due to low yield.

Table 3 gives the K_m, k_{cat} and calculated catalytic efficiency (k_{cat}/K_m). There was a relative invariance in K_m for all enzymes except for R59S and R59I, which had an approximately twofold lower affinity for the substrate. As in the case of their specific activities, the catalytic efficiencies of Y348C and R168C were lower than wild type (7% and 14% of wild type, respectively), but higher than R59W. The study of the catalytic efficiency on R59 mutants showed 44% of wild type for R59K, 1.4% of wild type for R59S and 1% of wild type for R59I. R59W had the lowest catalytic efficiency.

Our findings of severely reduced k_{cat}s and relatively invariant K_ms for R168C and R59W are in agreement with the findings of Dailey and Dailey [44].

In the study of the relevance of the R59, the introduction of both a conservative R59K and two nonconservative replacements, R59S and R59I, showed almost complete loss of PPOX activity for nonconservative substitutions, underlining the requirement of a positive charge in codon 59. This suggests, at least in part, a substrate binding problem in R59 mutants rather than a simple mechanistic problem.

3.4. Kinetics of PPOX inhibition

The inhibition of PPOX was studied using the inhibitors AF, MeAF, BV and BR. The IC_{50}s of PPOX for the various inhibitors and calculated Ki's for AF are shown in Table 4. When K_i was determined, increasing concentrations of AF increased the Km for protoporphyrinogen IX, while the V_{max} remained constant (data not shown), indicating competitive inhibition. α values of infinity calculated from the secondary replots confirmed this mode of inhibition. This is in keeping with earlier studies performed on human PPOX in lymphoblast sonicates [20]. We were able to compare the K_i values determined from the secondary replots with those calculated from the experimental IC_{50} data. These values correlated well, confirming the internal consistency of the model.

As in previous studies, the DPEs were good inhibitors of wild-type PPOX. However, Y348C and R168C mutants are less sensitive to inhibition by AF and MeAF compared to wild type and R59W. R59K and R59S mutants are less sensitive to inhibition by AF when compared to their counterpart R59I. The fact that the behaviour in the presence of these inhibitors does not parallel the observed differences in activity parameters may indicate that the inhibitor is binding near the active site rather than at the active site.

Inhibition by the haem degradation product, BV, was in contrast to the effects of AF and MeAF. Wild-type PPOX was relatively insensitive to inhibition by BV, whereas R59W was more sensitive by approximately 50%, and in the case of Y348C and R168C, a marked increase in sensitivity was apparent (Table 4).

The other haem degradation product, BR, did not inhibit wild-type PPOX nor any clinical mutants except Y348C where the inhibition was weak. Interestingly, this mutant was the only one that was unable to be stabilised by AF in

Table 4
IC_{50}s and calculated K_is for wild-type and mutant PPOXs

PPOX	IC_{50} (μM)				Calculated K_i (μM)
	AF	MeAF	BV	BR	AF
Wild type	4.20 ± 0.39	0.18 ± 0.01	41.00 ± 1.80	No inhibition	0.23 ± 0.02
Y348C	70.00 ± 4.30	55.60 ± 2.60	3.10 ± 0.35	34.20 ± 3.80	4.72 ± 0.28
R168C	46.00 ± 4.40	1.10 ± 0.08	0.40 ± 0.02	No inhibition	3.00 ± 0.26
R59W	4.20 ± 0.33	0.20 ± 0.03	21.00 ± 0.96	No inhibition	0.33 ± 0.02
R59K	3.33 ± 0.24	ND	ND	ND	0.18 ± 0.01
R59S	2.67 ± 0.19	ND	ND	ND	0.27 ± 0.02
R59I	0.90 ± 0.01	ND	ND	ND	0.11 ± 0.00
G14A	5.70 ± 0.22	ND	ND	ND	0.31 ± 0.01

ND = not determined.

thermal induced unfolding studies (see below). Differences in sensitivity to BV and BR have been ascribed to differences in rigidity between the two structures, BR being more convoluted and rigid than BV [23].

3.5. FAD binding

PPOXs contain a FAD cofactor that participates in a redox reaction during catalysis [10,12,16,19]. UV/VIS spectra were recorded for FAD standard, purified wild-type, and mutant PPOXs. The spectra for wild type and mutants R168C, Y348C, R59K, R59S, R59I and G14A were similar. All PPOXs except for R59W showed FAD-type spectra with absorption maxima at 375 and 450 nm. Fig. 1 shows the absorption maxima at 450 nm expressed per mg of protein giving an indication of the amount of FAD bound/not bound. The UV/VIS spectrum of R59W PPOX is different from that of wild type and all other mutants, indicating that FAD interaction with the protein is compromised. The low OD_{450}/mg/ml (Fig. 1) confirms this.

The effect of replacements in R59 on FAD binding have been discussed above (see PPOX activity) and reduced FAD binding in the R59W mutant confirms earlier studies of Dailey and Dailey [53].

Considering the FAD and activity data together, the R59W mutant had both severely compromised activity and FAD binding, while the R59S and R59I mutants (uncharged replacements) had reduced activity yet maintained FAD binding, and the R59K (positive charge replacement) had some activity and bound FAD, strongly suggesting that the positive charge at position 59 is required for catalytic activity and not FAD binding.

3.6. Effects of temperature on PPOX activity

To examine the effect of temperature on wild-type and mutant PPOX activity, T1/2 was measured. Fig. 2 shows typical activity curves obtained during denaturation of wild type and mutants. Generally there was a decrease in enzyme activities at temperatures over 45 °C except for R168C which was affected from 40 °C.

Table 5
$T_{1/2}$s of wild-type and mutant PPOXs

PPOX	$T_{1/2}$ (°C)
R59S	60.3 ± 0.33
G14A	57.0 ± 0.22
Wild type	56.8 ± 0.47
R59K	56.3 ± 0.47
R59I	54.2 ± 0.25
R59W	53.0 ± 0.71
Y348C	50.2 ± 0.43
R168C	47.6 ± 0.51

$T_{1/2}$s are shown in Table 5. The $T_{1/2}$ values of R59K and G14A are similar to that of wild type. Y348C, R59W, R168C and R59I have reduced $T_{1/2}$ values, and $T_{1/2}$ for R59S is increased. The effects of increasing temperature on the enzymatic activity of PPOX varied. Reduced $T_{1/2}$ values (for Y348C, R168C, R59W and R59I) and increased $T_{1/2}$ values (for R59S) suggest that these mutations have an influence on the structure of the active site.

R59W had a reduced $T_{1/2}$. A conservative replacement (R59K) resulted in a similar $T_{1/2}$ to that of the wild type whereas an aliphatic (R59I) substitution had a similar $T_{1/2}$ to that of R59W. A polar substitution (R59S) increased $T_{1/2}$ considerably, indicating that alteration in polarity at R59 is an important factor in the active site environment. This supports our previous suggestions, based on kinetic and FAD-binding data, that R59 is directly involved in catalysis and not simply important for FAD binding.

3.7. Thermal induced denaturation

In order to obtain qualitative information about the effect of the substitutions on stability and folding mechanisms, we compared the folding thermodynamic properties of mutant PPOXs to that of wild type.

The thermal equilibrium transition curves were determined by measuring absorbance at 270 nm. The melting

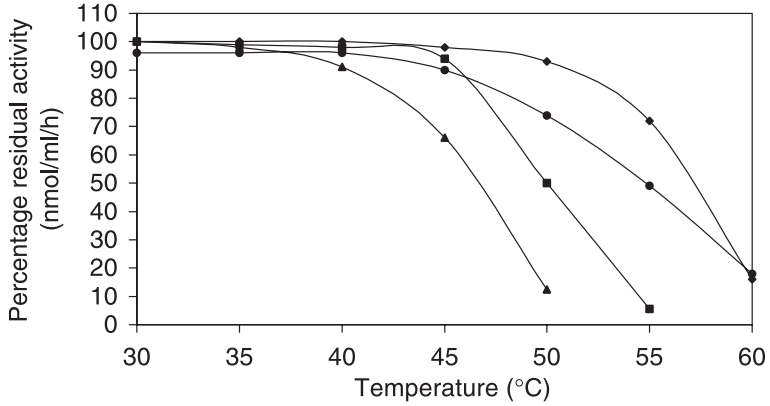

Fig. 2. Temperature induced reduction in activity of wild type (■), R59W (●), R168C (▲) and Y348C (♦) showing the effects of temperature on their activity. Curves for R59K, R59S, R59I and G14A are not shown, and they all fall between wild type and R59W.

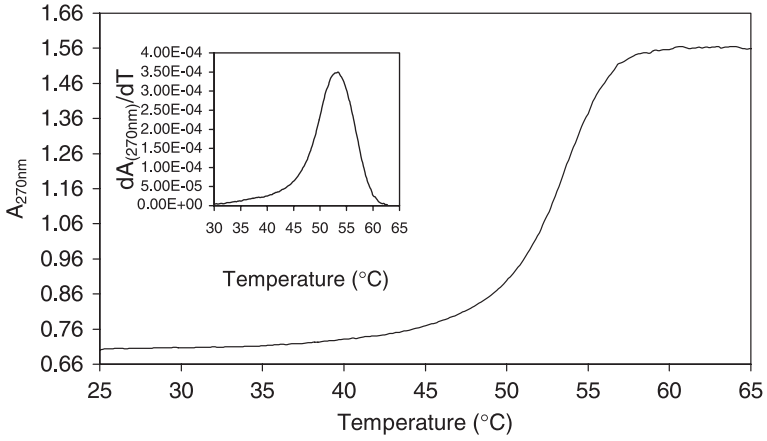

Fig. 3. Equilibrium transition curve for thermal unfolding of wild-type PPOX. The net stability of PPOX was determined from T_m in the middle of the transition region. Inset shows the first derivative curve.

curves generated for all PPOXs (except R168C and Y348C) were monophasic and showed co-operative unfolding as seen in the wild type (Fig. 3). In both R168C and Y348C, the melting curves suggested the onset of melting reflects the beginning of the unfolding process, but once past the T_m, irreversible aggregation occurs leading to a continuous increase in absorbance.

The T_m values for wild type and mutants are shown in Fig. 4 (white bars). T_m values for Y348C, R168C and R59W were relatively invariant at approximately 50 °C, whereas R59K, R59S and R59I displayed higher melting temperatures at approximately 60 °C, indicating that the latter three mutants were generally more stable than the three former mutants and wild-type PPOXs. This increased enzyme stability is a disadvantage to enzyme function. During catalysis, enzyme binds the substrate and undergoes conformational change before releasing the product. If the structure is too rigid, this conformational change may not occur, thus making the substrate-binding site inaccessible.

Generally, the kinetics of unfolding was a single first-order reaction. The melting curve is characteristic for a two-state transition indicative of the equilibrium that holds between the native and unfolded PPOX protein. Because PPOX is a large molecule, it is reasonable to assume that it forms a multi-domain structure, and these domains could unfold via a two-state process, independently. Indeed, it has previously been shown in the yeast form of the protein that there are two domains [18]. R168C and Y348C mutants have the potential to form additional or non-native disulfide bonds that influence unfolding equilibrium. With these mutants, multi-equilibrium with other cysteine residues may exist on unfolding, favouring aggregation.

When PPOX (for both wild type and mutants) was denatured and reheated after cooling, there was no melting curve observed for the second heating process. Instead, aggregation of PPOX was apparent (data not shown). This higher-order reaction involves slow aggregation of PPOX on denaturing, making the overall unfolding irreversible.

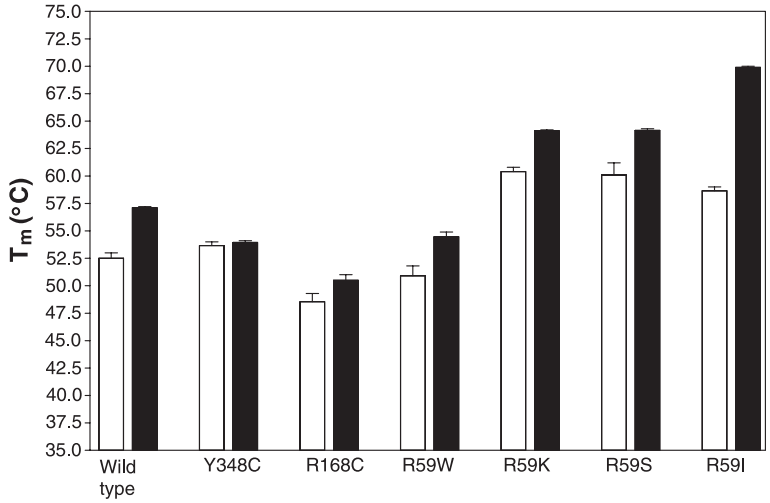

Fig. 4. Melting temperatures for wild-type and mutant PPOXs in the absence (white bars) and presence (black bars) of AF (protein/AF, 1:5).

When PPOX was heated to a temperature just below the T_m region, and slowly cooled back to a partially folded state (as seen by a higher absorbance), reheating to a fully unfolded state (denatured) showed a melting curve with co-operative unfolding. The T_m value of the partially folded PPOX was the same as for the fully folded structure (Fig. 5). The inset in Fig. 5 shows that unfolding started at a slightly higher temperature in the case of the partially folded structure. This effect was demonstrated for both wild-type and mutant PPOXs and shown to be the same. Thus, the first domain unfolds leaving another domain(s) folded. This partially unfolded structure is indicated by high absorbance, even after cooling to lower temperatures (15 °C), meaning that the protein does not become completely refolded. However, the remaining ordered structure maintains its stability and, on reheating, unfolds via a two-state mechanism. These domains remain undefined in any mammalian PPOX, but in the yeast form the two domains are defined in terms of a putative connecting loop, which corresponds to a specific protease cleavage site [18]. Furthermore, no PPOX crystal structure is available as yet.

DPE inhibitors have been observed to increase the thermostability of PPOX on addition of AF [60]. Hence, we investigated the effect of AF on the melting temperature by incubating them in the presence of the inhibitor, AF. The protein/AF ratio of 1:5 gave a maximum T_m and was used to compare protein stabilisation between wild type and mutants. The increase in T_m in the presence of AF was observed for the wild type and other mutants, except for R168C that had a small increase, and Y348C that had no increase (Fig. 4, black bars). The R59I mutant had the highest increase in T_m. This suggests that the inhibitor is "most comfortable" in the vicinity of a nonpolar side chain, as compared to the native arginine. The insensitivity of Y348C to all concentrations of AF tested suggests that alternative disulfide bridges which may be formed by this mutant, making the canonical AF binding site inaccessible. This is in agreement with our earlier findings (Table 4).

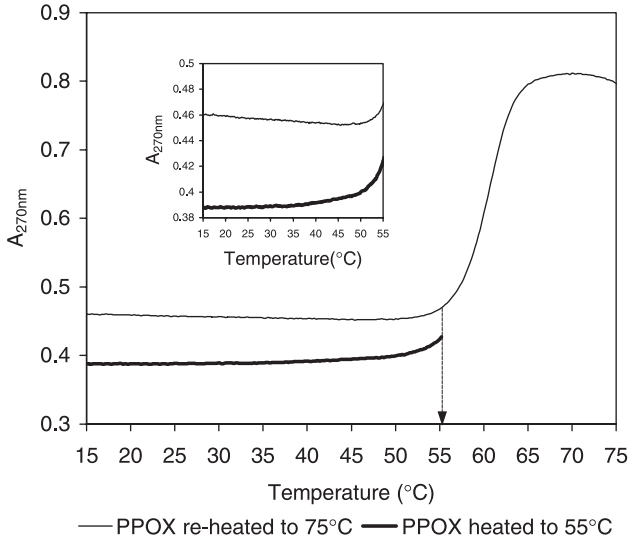

Fig. 5. Typical equilibrium transition curve for thermal unfolding of reheated PPOX (in this case wild type). The curves demonstrate partially folded PPOX with co-operative unfolding. An inset shows the region where heating was stopped (arrow) before reheating. The partially folded structure maintains its stability and starts unfolding at a slightly higher temperature.

As PPOX has a FAD cofactor, the proper folding of the native enzyme probably involves the correct assembly of the apoprotein with FAD. Previous work has shown that additional FAD (10–50 μM) increased the thermostability of PPOX marginally [60]. We also investigated the effect of FAD on the enzyme's stability. No significant increase in melting temperature of wild type and mutants was noted when incubated in the presence of increasing amounts of FAD (data not shown). Thus, assembly of PPOX holoprotein presumably involves many factors other than the simple introduction of FAD.

The observed data did not show any significant correlation between T_m and T1/2 values. T_m involves the overall structural stability while T1/2 reflect changes in the environment of the active site. The fact that there was no correlation in thermostability of these mutant PPOXs to their catalytic efficiency suggests that enzyme stability is not correlated to its activity in a simple way.

3.8. Secondary structural analysis

CD spectra of the wild-type and mutant PPOXs were recorded at 25 °C and analysed between wavelengths of 200 and 260 nm [61] as there was intense positive ellipticity below 200 nm (possibly due to the presence of FAD) and no useful information was obtained above 260 nm.

The CD spectra generated for wild-type PPOX showed a secondary structure with a dominating α-helix. The α-helix structure of the wild-type PPOX decreased to varying degrees for Y348C, R168C and R59W (Fig. 6) with increasing β-sheet and random coil structures. In contrast, R59K, R59S and R59I have severely decreased α-helical content with R59I having the most dramatic reduction. Generally, in all the mutants, β-sheet and random coil structures increased as α-helix decreased.

Earlier studies of yeast PPOX secondary structures [60] also showed α-helix as the dominating structure. In contrast, CD studies performed on murine PPOX [11] showed β-sheet as a dominating structure. These secondary structural differences are suggestive of the possibility of polymorphic structured PPOX.

As AF is a strong inhibitor of human PPOX and a possible stabilising influence on thermal denaturation, we attempted to study the effects of AF on the secondary structure of the protein. Our attempts proved unsuccessful even at protein/AF ratio of 1:0.5, probably due to the high intense positive ellipticity of the inhibitor and the fact that AF is difficult to maintain in solution.

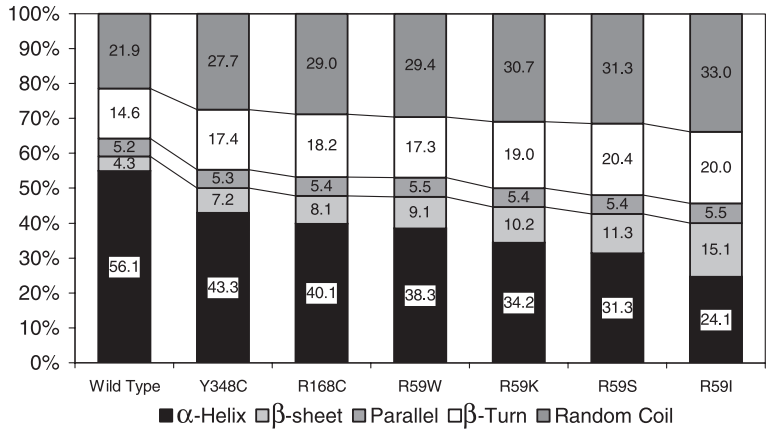

Fig. 6. Percentage secondary structures of wild-type and mutant PPOXs obtained from CD spectra.

3.9. Influence of R59W on PPOX structure/function

R59W had a reduced $T_{1/2}$. A conservative replacement (R59K) resulted in a similar $T_{1/2}$ to that of the wild type whereas an aliphatic (R59I) substitution had a similar $T_{1/2}$ to that of R59W. A polar substitution (R59S) increased $T_{1/2}$ considerably, indicating that alteration in polarity at R59 is an important factor in the active site environment. This supports our kinetic data, which suggest that R59 is directly involved in catalysis and not simply important for FAD binding.

Thermal equilibrium studies showed an increased T_m when mutating the R59. This increased thermostability suggests that the overall structure of the protein is affected when replacing this arginine. Seeing that R59 appears important at the active site as well, it is therefore possible to speculate that flexibility and/or charge distribution at the active site could be important for catalysis.

Secondary structure analysis of the R59 mutants reveals that the degree of α-helix present does not correlate linearly with the $T_{1/2}$ nor the T_m values, again supporting the assumption that R59 is important for catalysis at the active site. If the effects were purely structural, it could be expected that the structure/function relationship would correlate consistently.

Further studies will be necessary to fully understand the structure/function relationship underlying both normal and impaired PPOX activity as well as the stereochemistry and mechanism of the oxidation reaction. This study does, however, shed light on the role of the positive charge at R59, which appears to be directly involved in catalysis and not simply for FAD binding.

Acknowledgements

We express our thanks to Professor Harry Dailey (Biomedical and Health Sciences Institute of Georgia, Athens, GA, USA) for providing us with the pHPPOX vector and the R168C mutant, and Madhu Chauhan (Molecular and Cell Biology, University of Cape Town) for her technical assistance in running the CD spectra. This project was financed in part by the Wellcome Trust under their International Senior Research Fellowship program in which Peter Meissner is the recipient of a Wellcome Senior Fellowship for Medical Science in South Africa.

References

[1] R. Poulsen, W.J. Polglase, The enzymic conversion of protoporphyrinogen IX to protoporphyrin IX. Protoporphyrinogen oxidase activity in mitochondrial extracts of *Saccharomyces*, J. Biol. Chem. 250 (1975) 1269–1274.

[2] H.A. Dailey, Conversion of coproporphyrin to protoheme in higher eukaryotes: terminal three enzymes, in: H.A. Dailey (Ed.), Biosynthesis of Haem and Chlorophylls, McGraw-Hill, New York, 1990, pp. 123–161.

[3] J.-M. Camadro, F. Thome, N. Brouillet, P. Labbe, Purification and properties of protoporphyrinogen oxidase from the yeast *Saccharomyces cerevisiae*. Mitochondrial location and evidence for a precursor form of the protein, J. Biol. Chem. 269 (1994) 32085–32091.

[4] D.J. Klemm, L.L. Barton, Oxidation of protoporphyrinogen in the obligate anaerobe *Desulfovibrio gigas*, J. Bacteriol. 164 (1985) 316–320.

[5] G.C. Ferreira, T.A. Andrew, S.W. Karr, H.A. Dailey, Organisation of the terminal two enzymes of the heme biosynthetic pathway, J. Biol. Chem. 263 (1988) 3825–3839.

[6] H.A. Dailey, T.A. Dailey, Protoporphyrinogen oxidase of *Myxococcus xanthus*. Expression, purification, and characterization of the cloned enzyme, J. Biol. Chem. 271 (1996) 8714–8718.

[7] C. Jones, P.M. Jordan, M. Akhtar, Mechanism and stereochemistry of the porphobilinogen deaminase and protoporphyrinogen IX oxidase reaction: stereospecific manipulation of hydrogen atoms at the four methylene bridges during the biosynthesis of haem, J. Chem. Soc., Perkin Trans. 1 (1984) 2625–2633.

[8] M. Akhtar, Mechanism and stereochemistry of the enzymes involved in the conversion of uroporphyrinogen III into haem, in: P.M. Jordan (Ed.), Biosynthesis of Tetrapyrroles, Elsevier, Amsterdam, 1991, pp. 67–99.

[9] T.A. Dailey, H.A. Dailey, Identification of an FAD superfamily containing protoporphyrinogen oxidases, monoamine oxidases, and phytoene desaturase, J. Biol. Chem. 273 (1998) 13658–13662.

[10] H.A. Dailey, S.W. Karr, Purification and characterization of murine protoporphyrinogen oxidase, Biochemistry 26 (1987) 2697–2701.
[11] K.L. Proulx, H.A. Dailey, Characteristics of murine protoporphyrinogen oxidase, Protein Sci. 1 (1992) 801–809.
[12] L.J. Siepker, M. Ford, R. de Kork, S. Kramer, Purification of bovine protoporphyrinogen oxidase: immunological cross-reactivity and structural relationship to ferrochelatase, Biochim. Biophys. Acta 913 (1987) 349–358.
[13] J.M. Jacobs, J.N. Jacobs, Oxidation of protoporphyrinogen to protoporphyrin, a step in chlorophyll and haem biosynthesis: purification and partial characterization of the enzyme from barley organelles, Biochem. J. 244 (1987) 219–224.
[14] A. De Marco, S. Volrath, T. Bruyere, M. Law, R. Fonné-Pfister, Recombinant maize protoporphyrinogen IX oxidase expressed in *Escherichia coli* forms complexes with GroEL and DnaK chaperones, Protein Expr. Purif. 20 (2000) 81–86.
[15] N. Watanabe, F. Che, K. Terashima, S. Takayama, S. Yoshida, A. Isogai, Purification and properties of protoporphyrinogen oxidase from spinach chloroplasts, Plant Cell Physiol. 41 (2000) 889–892.
[16] T.A. Dailey, H.A. Dailey, Human protoporphyrinogen oxidase: expression, purification and characterization of the cloned enzyme, Protein Sci. 5 (1996) 98–105.
[17] K. Nishimura, S. Taketani, H. Inokuchi, Cloning of a human cDNA for protoporphyrinogen oxidase by complementation in vivo on a *hemG* mutant of *Escherichia coli*, J. Biol. Chem. 270 (1995) 8076–8080.
[18] S. Arnould, J.-M. Camadro, The domain structure of protoporphyrinogen oxidase, the molecular target of diphenyl ether-type herbicides, Proc. Natl. Acad. Sci. U. S. A. 95 (1998) 10553–10558.
[19] J.-M. Camadro, M. Matringe, R. Scalla, P. Labbe, Kinetic studies on protoporphyrinogen oxidase inhibition by diphenyl ether herbicides, Biochem. J. 277 (1991) 17–21.
[20] A.V. Corrigall, R.J. Hift, P.A. Adams, R.E. Kirsch, Inhibition of mammalian protoporphyrinogen oxidase by acifluorfen, Biochem. Mol. Biol. Int. 34 (1994) 1283–1289.
[21] J.M. Jacobs, N.J. Jacobs, S.E. Borotz, M.L. Guerinot, Effects of photobleaching herbicide, acifluorfen methyl, on protoporphyrinogen oxidation in barley organelles, soybean root mitochondria, soybean root nodules, and bacteria, Arch. Biochem. Biophys. 280 (1990) 369–375.
[22] T.A. Dailey, P.N. Meissner, H.A. Dailey, Expression of a cloned protoporphyrinogen oxidase, J. Biol. Chem. 269 (1994) 813–815.
[23] A.V. Corrigall, K.B. Siziba, M.H. Maneli, E.G. Shephard, M. Ziman, T.A. Dailey, H.A. Dailey, R.E. Kirsch, P.N. Meissner, Purification of and kinetic studies on a cloned protoporphyrinogen oxidase from aerobic bacterium *Bacillus subtilis*, Arch. Biochem. Biophys. 358 (1998) 251–256.
[24] N. Watanabe, F. Che, M. Iwano, S. Takayama, T. Nakano, S. Yoshida, A. Isogai, Molecular characterization of photomixotrophic tobacco cells resistant to protoporphyrinogen oxidase-inhibiting herbicides, Plant Physiol. 118 (1998) 751–758.
[25] I. Lermontova, B. Grimm, Overexpression of plastidic protoporphyrinogen IX oxidase leads to resistance to diphenyl-ether herbicide acifluorfen, Plant Physiol. 122 (2000) 75–83.
[26] G.C. Ferreira, H.A. Dailey, Mouse protoporphyrinogen oxidase. Kinetic parameters and demonstration of inhibition by bilirubin, Biochem. J. 250 (1988) 597–603.
[27] D.A. Brenner, J.R. Bloomer, The enzymatic defect in variegate porphyria, N. Engl. J. Med. 302 (1980) 765–769.
[28] J.Ch. Deybach, H. de Verneuil, Y. Nordmann, The inherited defect in porphyria variegata, Hum. Genet. 58 (1981) 425–428.
[29] P.N. Meissner, R.S. Day, M.R. Moore, P.B. Disler, E. Harley, Protoporphyrinogen oxidase and porphobilinogen deaminase in variegate porphyria, Eur. J. Clin. Investig. 16 (1986) 257–261.
[30] R.S. Day, Variegate porphyria, Semin. Dermatol. 5 (1986) 138–154.
[31] P.N. Meissner, T.A. Dailey, R.J. Hift, M. Ziman, A.V. Corrigall, A.G. Roberts, D.M. Meissner, R.E. Kirsch, H.A. Dailey, A R59W mutation in human protoporphyrinogen oxidase results in decreased enzyme activity and is prevalent in South Africans with variegate porphyria, Nat. Genet. 13 (1996) 95–97.
[32] L. Warnich, M.J. Kotze, I.M. Groenewald, J.Z. Groenewald, M.G. van Brakel, C.J. van Heerden, J.N.P. de Villiers, W.J.M. van de Ven, E.F.P.M. Shoenmakers, S. Taketani, A.E. Retief, Identification of the three mutations and associated haplotypes in the protoporphyrinogen oxidase gene in South African families with variegate porphyria, Hum. Mol. Genet. 5 (1996) 981–984.
[33] A.V. Corrigall, R.J. Hift, V. Hancock, D. Meissner, L. Davids, R.E. Kirsch, P.N. Meissner, Identification and characterisation of a deletion (537delAT) in the protoporphyrinogen oxidase gene in a South African variegate porphyria family, Human Mutat. 12 (1998) 403–407.
[34] A.V. Corrigall, R.J. Hift, L.M. Davids, V. Hancock, D. Meissner, R.E. Kirsch, P.N. Meissner, Homozygous variegate porphyria in South Africa: genotypic analysis in two cases, Mol. Genet. Metab. 69 (2000) 323–330.
[35] A.V. Corrigall, R.J. Hift, L.M. Davids, V. Hancock, D. Meissner, R.E. Kirsch, P.N. Meissner, Identification of the first variegate porphyria mutation in an indigenous black South African and further evidence for heterogeneity in variegate porphyria, Mol. Genet. Metab. 73 (2001) 91–96.
[36] S.D. Whatley, H. Puy, R.R. Morgan, A.M. Robreauw, A.G. Roberts, Y. Nordmann, G.H. Elder, J.-C. Deybach, Variegate porphyria in Western Europe: identification of PPOX gene mutation in 104 families, extent of allelic heterogeneity, and absence of correlation between phenotype and type of mutation, Am. J. Hum. Genet. 65 (1999) 984–994.
[37] N. Maeda, Y. Horie, Y. Sasaki, K. Adachi, E. Nanba, K. Nishida, R. Saigo, M. Nakagawa, Three novel mutations in the protoporphyrinogen oxidase gene in Japanese patients with variegate porphyria, Clin. Biochem. 33 (2000) 495–500.
[38] M. von und zu Fraundberg, R. Tenhunen, R. Kauppinen, Expression and characterization of six mutations in the protoporphyrinogen oxidase gene among Finnish variegate porphyria patients, Mol. Med. 7 (2001) 320–328.
[39] J. Frank, F.K. Jugert, H.K. Merk, K. Kalka, G. Goerz, K. Anderson, D.R. Bickers, M.B. Poh-Fitzpatrick, A.M. Christiano, A spectrum of novel mutations in the protoporphyrinogen oxidase gene in 13 families with variegate porphyria, J. Invest. Dermatol. 116 (2001) 821–823.
[40] J. Frank, V.M. Aita, W. Ahmad, H. Lam, C. Wolff, A.M. Christiano, Identification of a founder mutation in the protoporphyrinogen oxidase gene in variegate porphyria patients from Chile, Hum. Hered. 51 (2001) 160–168.
[41] A.G. Roberts, S.D. Whatley, J. Daniels, P. Holmans, I. Fenton, M.J. Owen, P. Thompson, C. Long, G.H. Elder, Partial characterization and assignment of the gene for protoporphyrinogen oxidase and variegate porphyria to human chromosome 1q23, Hum. Mol. Genet. 4 (1995) 2387–2390.
[42] S. Taketani, J. Inazawa, T. Abe, T. Furukawa, H. Kohno, R. Tokunaga, K. Nishimura, H. Inokuchi, The human protoporphyrinogen oxidase (PPOX) gene: organisation and localisation to chromosome 1, Genomics 29 (1995) 698–703.
[43] H. Puy, A.M. Robreau, R. Rosipal, Y. Nordmann, J.C. Deybach, Protoporphyrinogen oxidase: complete genomic sequence and polymorphisms in the human gene, Biochem. Biophys. Res. Commun. 226 (1996) 226–230.
[44] H.A. Dailey, T.A. Dailey, Characteristics of human protoporphyrinogen oxidase in controls and variegate porphyria, Cell. Mol. Biol. 43 (1997) 67–73.
[45] A.G. Roberts, H. Puy, T.A. Dailey, R.R. Morgan, S.D. Whatley, H.A. Martasek, P. Martasek, Y. Nordmann, J. Deybach, G.H. Elder, Molecular characterization of homozygous variegate porphyria, Hum. Mol. Genet. 7 (1998) 1921–1925.
[46] R.R. Morgan, V. Da Silva, H. Puy, G.H. Elder, Functional studies of

mutations in the human protoporphyrinogen oxidase gene in variegate porphyria, Cell. Mol. Biol. 48 (2002) 79–82.
[47] T.A. Dailey, H.A. Dailey, P. Meissner, A.R.K. Prasad, Cloning, sequencing, and expression of mouse protoporphyrinogen oxidase, Arch. Biochem. Biophys. 324 (1995) 379–384.
[48] U.K. Laemmli, Cleavage of structural proteins during the assembly of head of bacteriophage T4, Nature (Lond.) 277 (1970) 680–685.
[49] M. Bradford, A rapid and sensitive method for quantitation of microgram quantities of protein utilising the principle of protein–dye binding, Anal. Biochem. 72 (1976) 248–254.
[50] L.A. Marky, K.J. Breslauer, Calculating thermadynamic data for transitions of any molecularity from equilibrium melting curves, Biopolymers 26 (1987) 1601–1620.
[51] G. Deléage, B. Roux, An algorithm for protein secondary structure prediction based on class prediction, Protein Eng. 1 (1987) 289–294.
[52] J.F. Kane, D.L. Hartley, Formation of recombinant protein inclusion bodies in *Escherichia coli*, TIBTECH 6 (1988) 95–101.
[53] T.A. Dailey, H.A. Dailey, Expression, purification and characterization of mammalian protoporphyrinogen oxidase, Methods Enzymol. 281 (1997) 340–349.
[54] S. Arnould, M. Takahashi, J.-M. Camadro, Acylation stabilizes a protease-resistant conformation of protoporphyrinogen oxidase, the molecular target of diphenyl ether-type herbicides, Proc. Natl. Acad. Sci. U. S. A. 96 (1999) 14825–14830.
[55] H. Tian, L. Yu, M.W. Mather, C.A. Yu, The flexibility of the neck region of the rieske iron sulfur protein is functionally important in the cytochrome bc_1 complex, J. Biol. Chem. 273 (1998) 27953–27959.
[56] R.K. Wierenga, P. Terpstra, W.G.J. Hol, Prediction of the occurrence of the ADP-binding βαβ-fold in proteins, using an amino acid sequence fingerprint, J. Mol. Biol. 187 (1986) 101–107.
[57] A. Vrielink, L.F. Lloyd, D.M. Blow, Crystal structure of cholesterol oxidase from *Brevibacterium sterolicum* refined at 1.8 Å resolution, J. Mol. Biol. 219 (1991) 533–554.
[58] D.L. Roberts, F.E. Frerman, J.P. Kim, Three dimensional structure of human electron transfer flavoprotein to 2.1-Å resolution, Proc. Natl. Acad. Sci. 93 (1996) 14355–14360.
[59] Y. Nishiya, T. Imanaka, Analysis of interaction between the *Arthrobacter* sarcosine oxidase and the coenzyme flavin adenine dinucleotide by site-directed mutagenesis, Appl. Environ. Microbiol. 62 (1996) 2405–2410.
[60] S. Arnould, M. Takahashi, J.-M. Camadro, Stability of recombinant yeast protoporphyrinogen oxidase: effect of diphenyl ether-type herbicides and diphenyleneiodonium, Biochemistry 37 (1998) 12818–12828.
[61] J.P. Hennessey , W.C. Johnson Jr., Information content in the circular dichroism of proteins, Biochemistry 20 (1981) 1085–1094.